Indian Journal of Biochemistry & Biophysics
Vol. 63, June 2026, pp. 678-688
DOI: 10.56042/ijbb.v63i6.24813

Prospective neuro-muscular protection of Theaflavin gallate and tea extract by suppressing acetylcholinesterase in rat, verified by *in vitro* and MD simulation studies

Tanmoy Samanta[1]*, Amrita Banerjee[2], Krishna Somaletha Chandran[1], Nandita Medda[3], Aniket Sarkar[3], Anindya Sundar Panja[3], Adinpunya Mitra[1], Subrata Kr. De[4] & Smarajit Maiti[5]*

[1]Natural Product Biotechnology Group, Agricultural and Food Engineering Department, Indian Institute of Technology Kharagpur, Kharagpur-721 302, West Bengal, India

[2]Centre for Industrial Biotechnology, Research, Siksha 'O' Anusandhan Deemed to be University, Kalinganagar, Bhubaneswar-751 030, Odisha, India

[3]Department of Biochemistry and Biotechnology, Oriental Institute of Science and Technology, Midnapore-721 102, West Bengal, India

[4]Department of Zoology, Vidyasagar University, Medinipur-721 102, West Bengal, India

[5]Haldia Institute of Health Sciences, ICARE Complex, Hatiberia, Haldia-721 657, Purba Medinipur, West Bengal, India

Received 14 October 2025; *revised 01 April 2026*

Possible therapeutic interventions of acetylcholinesterase induction were studied. Inhibition of AChE might be helpful in treating the neuro-muscular diseases. Over-expressions of acetylcholinesterase (AChE), a key regulation of the neurotransmitter acetylcholine influences some neurodegenerative/neuro-muscular disorders. Present study evaluated the effect of black-tea components on AChE-activity in *in vitro,* and *in vivo i.e.* arsenic-intoxicated (0.6ppm/day/4-weeks) rat brain-AChE inhibition. Inhibitory-effects and enzyme kinetics on purified-AChE were screened from ten pure tea-phytochemicals. *In vivo* experiment and bioinformatics studies were also performed. Pure theaflavin-digallate and theaflavin-monogallate showed promising AChE inhibitory effects/kinetics in dose-dependent/mixed-type manner with IC_{50} values, 1.6 µM and 3.3 µM, respectively. Tea galloyl-ester catechins compounds inhibited AChE with IC_{50} values of 41-67 µM. Arsenic exposure increased AChE activity in rat cerebellum which was significantly restored by black-tea paralleling with our *in vitro* results. Molecular-docking and MD-simulation (GROMACS2021.2 server) of AChE (PDB Id:4M0E) and the experimental compounds suggests that theaflavin-digallate showed the lowest Atomic-Contact-Energy -369.87 kcal/mol and hampers the enzyme catalytic-hydrolytic-action and nucleophilic attack by SER203 supporting the *in vitro* and animal experimental results. Compared to other flavonoid or positive-control inhibitor eserine sulfate, TFDG and TFMG demonstrated significant inhibition of AChE. In conclusion, current MD-simulation, *in vitro*, and in vivo data may help treat certain cholinergic diseases. Further studies are suggested.

Keywords: Acetylcholinesterase, Arsenic-intoxication, Molecular docking, Neurodegenerative and muscular disorders, Tea phytochemicals

In mammalian nerve cells, acetylcholinesterase (AChE) controls the quantity of acetylcholine at the synapse by hydrolyzing the neurotransmitter. The cholinergic system is involved in memory and learning[1]. The first chemical to be identified as a neurotransmitter that transmits messages from the brain to muscles is acetylcholine (ACh). The main goal of AChE inhibition was to address neurological issues. One of the most prevalent causes of dementia in people over 65 is Alzheimer's disease (AD), in which cholinergic activity declines, leading to age-related cognitive impairment and dementia. AD accounts for 50% to 60% of all cases of dementia[2]. Besides treating AD, AChE inhibition is also targeted in the treatment of myasthenia gravis[3]. Acetylcholine (ACh) is degraded quickly at the neuromuscular junction, which is the main reason why high acetylcholinesterase (AChE) activity can cause neuromuscular diseases. So, the ability of ACh to bind to and activate muscle receptors become restricted by this quick breakdown, which impairs muscular contraction and causes weakness[4].

ACh metabolism and aberrant AChE expression have been linked to a number of neuromuscular conditions, including inflammatory myopathies, Guillain-Barré syndrome, and Duchenne muscular dystrophy. One of the many diverse roles of the

*Correspondence:
E-mail: smarajitmaiti69@gmail.com (SM);
tana.biochem@gmail.com (TS)
Suppl. data available on respective page of NOPR

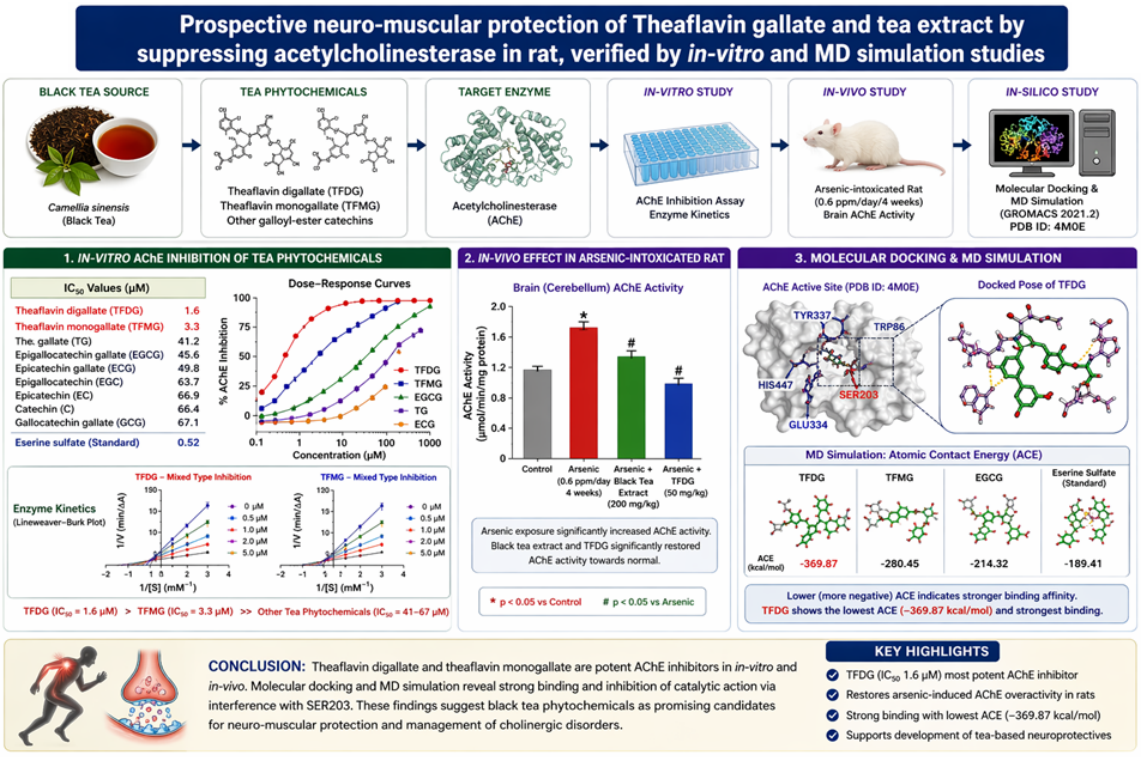

Graphical abstract

enzyme AChE is its morphogenic activity. As the nervous system develops, AChE is in charge of axon growth, thalamocortical connections, and the formation of neuromuscular junctions. Changes in cell architecture during neurogenesis may be mediated by AChE[5]. Therefore, in relevant clinical conditions; attacking AChE has proven an appealing option. AChE activity has been inhibited by a variety of synthetic, chemical, and phytochemical agents at various points in time.

Recently, three facets of AChE ligand design have drawn a lot of interest. These include variants of the well-known AChE ligand, scaffolds composed of natural materials, and multifunctional ligands. Although new AChE inhibitors with polypharmacology or dual inhibitory action have also been discovered, most of them only show weak micromolar efficacy[6]. Alzheimer's disease is now treated using cholinesterase (AChE and Butyrylcholinesterase BuChE) inhibitors, including galantamine, tacrine, donepezil, physostigmine, and rivastigmine[7-9].

However, these compounds have side effects such as hepatotoxicity[9,10]. For this study, an *in vivo* AChE regulation model experiment may be useful. Several reports including some of our previous work suggests that arsenic can damage brain tissues with concomitant increase of AChE[10,11]. Additionally, epidemiological evidence suggests that arsenic causes neurobehavioral deficits such as movement disorder[12,13]. According to reports, some phytochemicals may prevent animals inebriated by arsenic by suppressing cholinesterase[14]. The high concentration of polyphenols, such as theaflavins and catechins, which have been shown to have anti-carcinogenic properties, is primarily responsible for the health advantages of tea extract[15]. The phytochemicals in black tea that regulate AChE have not been thoroughly studied. Compared to green tea, black tea has more theaflavins[16]. We show that theaflavin gallate has a strong inhibitory effect on acetylcholinesterase activity.

Assessing the regulatory effects of tea polyphenols on AChE activity and estimating the medicines' effective concentration in the regulation process were the main goals of the current study. We postulated that inhibition of AChE might limit ACh depletion, which would be advantageous for some neuromuscular and other illnesses, based on our prior findings and other published papers. Furthermore, as was previously said, tea polyphenols would be less likely to have adverse effects and other health problems than other medications. Here, we

investigated the effect of black tea on an arsenic-intoxicated rat model where arsenic significantly enhanced ACHE activity. We evaluated *in vitro* inhibitory effects of pure-phytochemicals like theaflavins, catechins and their derivatives on pure-AChE. We conducted bioinformatics, docking and molecular-dynamic simulation studies to verify phytochemicals-AChE binding stability. In light of all these findings, we propose that theaflavins may have an AChE-inhibitory and potentially neuroprotective function. This work is significant since it identifies several strong tea phytochemicals that may have a role in inhibiting AChE. It might be more readily available and have fewer adverse effects than synthetic chemicals or medications.

Materials and Methods

The present study is reported in accordance with ARRIVE guidelines (https://arriveguidelines.org).

Reagents and Chemicals

The tea biochemical compounds used for this study were purchased from Sigma-Aldrich (Saint Louis, Missouri, USA). These were EC, EGC, CG, ECG, EGCG, GCG, TF, TFMG, TFDG and gallic acid (GA). AChE type VI-S (from electric eel), Acetylthiocholine iodide (ATCI) and 5,5′-dithiobis [2-nitrobenzoic acid] (DTNB) were purchased from Sigma.

In vivo experiment in arsenic intoxicated rat model

Preparation of Black Tea Extract

Extractives of black tea (obtained from the Tea Research Centre, Agricultural and Food Engineering Department, Indian Institute of Technology Kharagpur, India) were prepared by boiling 9 g of respective samples in 375 mL water for 5 min followed by filtration (using Whatman No. 1 filter paper). Black tea extractives were then freeze dried at -40°C for two days before being refrigerated for future use.

Preparation of Arsenic Solution

For this experiment, Sodium-meta-arsenite ($NaAsO_2$) was used as an arsenic source by dissolving it in distilled water, maintaining a 0.6 ppm concentration Different dose-response studies on arsenic exposure to rat were performed. This dose was selected due to its not being lethal for the animal, but the exposure of arsenic in an animal model for a moderate time period of 4 weeks or 28 days can generate toxicity in their body.

Treatment and Group Distribution of Animal Model

Rats were purchased from a government accredited CPCSEA-Committee farm house for the Purpose of Control and Supervision of Experiments on Animals: Reg. no. 1A2A/PO/BT/S/15/CPCSEA (http:// cpcsea.nic.in/Auth/index.aspx) organization under the Department of Animal Husbandry and Dairy, Ministry of Agriculture and Farmer's Welfare, Govt. of India. For all animal experiments, Institutional permission and ethical approval was obtained. We followed all ethical norms of Helsinki Declaration (2000) and NIH guidelines.

Female albino rats weighing 150±10g were acclimated to a pellet diet and water for 10 days at 32±2°C and 50–70% humidity. Three groups of four rats each were randomly assigned to their respective groups. The sole food given to the control/group I animals was drinking water. Animals in group II (arsenic-treated) were given 0.5 mL of arsenic in 0.6 ppm water for four weeks. Animal behavior and mobility were noted during the course of the treatment. Arsenic + black-tea treated/ Group-III animals were fed or 0.5 mL arsenic of 0.6 ppm + 0.5 mL of 1% (*w/v*) lyophilized black-tea extract (4-weeks)[17,13].

AChE Extraction and Partial Purification

Animals were exposed to light anesthesia (pentobarbital 40 mg/kg i.p). The cerebellum was dissected and stored at -40°C and homogenized in phosphate-buffer. A partially purified enzyme was separated on a discontinuous sucrose gradient. Brain re-suspension was carefully layered on top of the gradient and centrifuged at 25,000 × g for 3 h. Synaptosomes at the interphase were eluted by displacing the contents with 2M sucrose and its protein concentration was measured[18]. Partially purified enzyme was employed for enzyme-activity determination.

Acetylcholinesterase assay from rat cerebellum cytosol

Acetylcholinesterase was assayed by Ellman's method using DTNB as chromogen and acetylthiocholine iodide as substrate[17]. The extinction coefficient, = 13600 M^{-1} cm^{-1}, was used to calculate enzyme activity.

Acetylcholinesterase Inhibition Studies using pure form of Tea component

Acetylcholinesterase assay

Acetylcholinesterase was assayed using the above method except for one modification. Here, 100 μL of

0.086 U/mL AChE (from electric eel) was added to the reaction mixture instead of AChE extract from rat cerebellum. A standard solution of eserine salicylate was used as a positive control for the AChE inhibitor[17,19].

Determination of *AChE* inhibitory activity

Tea phytochemicals (pure) such as EC, EGC, ECG, EGCG, GCG, and CG used for inhibition studies with concentration; 5, 10, 20, 30, and 40 µg/mL. And TFDG, TFMG, and TF were used; 4, 6, and 8 µg/mL. Additionally, the concentrations of gallic acid were 100 to 500 µg/mL. The percentage of AChE inhibitory activity (% IA) was calculated by using the equation[31]: % IA = $[(A_c - A_t)/A_c] \times 100$, where, A_c is the activity of control enzyme (containing all reactants, except the tea components) and A_t is the activity of the tested compound. All experiments were performed in triplicate.

Estimation of IC_{50} values

The concentrations of the test samples that inhibited the hydrolysis of substrate (acetylthiocholine iodide) by 50% (IC_{50}) were determined by a linear regression analysis between the inhibition percentages against the log concentrations of inhibitors using the OriginPro 8 software (https://www.originlab.com/) and the Microsoft Office Excel 2007 program (https://microsoft-office-2007.en.lo4d.com/windows).

***Acetylcholinesterase* inhibition kinetics**

Kinetic studies of AChE inhibition were carried out using six concentrations (37.5, 75, 122.5, 150, 225, and 300 µM) of ATCI. A control set was carried out without any inhibitor. The control assay contained 100 µL of 0.086 U/mL AChE (from electric eel), 500 µL of DTNB (3 mM), and ATCI (37.5–300 µM). Two fixed concentrations (5 µM and 2.5 µM) of each inhibitor (TF, TFMG, and TFDG) were used to study inhibition kinetics. The Lineweaver–Burk equation was employed to determine K_m, V_{max}, and K_{cat} and catalytic-efficiency (K_{cat}/K_m). The correlation coefficient, slope, and intercept were obtained by linear regression analysis.

Histo-architecture and *Cytogenetic* essay

Analysis of rat *cerebellum* histology and *DNA* Comet Assay

Soon after the sacrifice, the cerebellum was removed and placed in fixative. These tissues were sectioned at 5 microns, embedded in a paraffin block, and stained with eosin and hematoxylin. Stained slides were examined under a light microscope (Nikon, Eclipse LV100, 10 X magnifications) for the histo-architectural investigation. Seventy five ml of low melting-point agarose (0.6%) was mixed with 25 mL of cell suspension (105 cells, cerebellum). Slides that had previously been coated with 1% agarose were covered with the mixture after a coverslip was placed. A gel electrophoresis chamber (Bio-Rad, USA) was used to hold the slides. The slides were viewed on a Nikon, Eclipse LV100 POL fluorescent microscope using VisComet software (ImpulsBildanalyze). Ghost cell formation, comet head/tail dimension, and head pixel density were used to examine the comet's character[17,13].

Protein and ligand structure retrieval and *molecular docking* study

An X-ray crystallographic structure of human acetylcholinesterase was retrieved from the Protein Data Bank (PDB ID: 4M0E). The removal of other molecules complexed with 4M0E was performed using BIOVIA Discovery Studio 2017R2 (https://discover.3ds.com/discovery-studio-visualizer-download). All the flavonoid structures were retrieved from the PubChem [https://pubchem.ncbi.nlm.nih.gov/] database. Different molecular docking of dihydrotanshinone, eserine, and other inhibitors like TFMG, TFDG etc. with acetylcholinesterase were performed by Autodock Tools -1.5.6 (The Scripps Research Institute (https://autodocksuite.scripps.edu/adt/)) and the PatchDock server [https://bioinfo3d.cs.tau.ac.il/Patch Dock/].

The grid box values during the Autodock run with acetylcholinesterase and substrate dihydrotanshinone were as follows: - X and Y-dimension: 96, Z- dimension: 118; Spacing (Å): 0.703; Center grid box (X center:1.498, offset: 4.417; Y center: -40.658, offset: -0.694 and Z center: 33.804, offset: 2.694). The 3D structure of the AChE control inhibitor eserine salicylate was not available in PubChem, so it was constructed and for docking with acetylcholinesterase. All the structures of ligand molecules were listed in (Suppl. Fig. S1).

Molecular dynamics (MD) simulation

The study utilized molecular dynamics simulations to investigate the behavior of two complex systems, revealing favorable interactions with acetylcholinesterase. These simulations extended over 100-nanosecond duration, employing the CHARMM27 force field[20] and adhering to thermodynamic conditions. Furthermore, the root

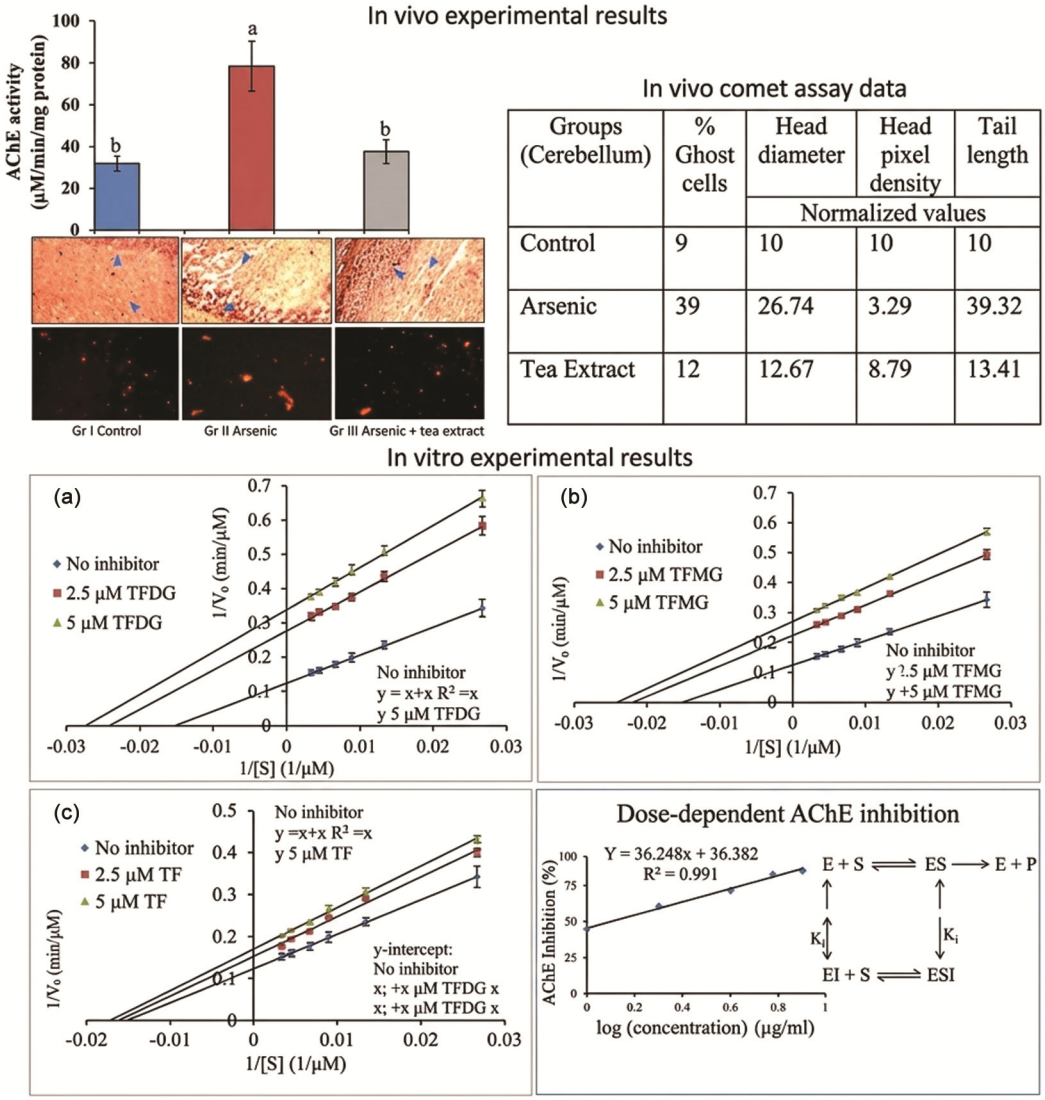

Groups (Cerebellum)	% Ghost cells	Head diameter	Head pixel density	Tail length
		Normalized values		
Control	9	10	10	10
Arsenic	39	26.74	3.29	39.32
Tea Extract	12	12.67	8.79	13.41

Fig. 1 — (upper panel) Comparative analysis of rat cerebellum AChE activities extracted from different treated rats. Values are represented as mean ± SD where n = 3. Mean values with same alphabetical letters are not significantly different at $P \leq 0.05$. Histo-architecture of the cerebellum are shown. The DNA stability data from Comet assay are presented. (lower panel) Lineweaver–Burk plot of AChE activity with different substrate concentrations (30–300 µM) in the absence and presence of 2.5 µM and 5 µM of (A) TFDG, (B) TFMG and (C) TF. In the bottom right panel IC_{50} value of TFMG has been determined in a graph presentation. Possible enzyme (E) substrate (S) reaction steps and product (P) formation has been shown

mean square fluctuation (RMSF) was computed to quantify individual atom fluctuations within the systems. The analysis of the simulation trajectory was performed using the GROMACS 2021.2 utility tool gmx-rms[21].

Analysis of Total Energy and Force Field

The trajectory generated during the molecular dynamics simulation was analyzed using the Swiss PDB Viewer (http://www.expasy.org/spdbv/). Total energy profiles and force field calculations were examined to assess the stability and interactions within the acetylcholinesterase (AChE) & Theaflavin monogallate (TFMG) complex as well as acetylcholinesterase & Theaflavin digallate (TFDG). This analysis provided insights into the binding affinity, structural changes, and potential binding pockets[22].

Results and Discussion

***Acetylcholinesterase* activity in rat cerebellum cytosol**

Four weeks of arsenic treatment in rat significantly increased the acetylcholinesterase activity in the rat cerebellum (Fig. 1). Arsenic-treated animals (Group

II) were found to be unstable and losing their balance. After three weeks, a certain degree of restlessness and vertigo was noticed in this group. In this regard, arsenic plus black tea protected the Group III rats and the AChE activity (Fig. 1). The restoration and reorganization of cerebellum tissue by tea extract were presented in earlier publication[13] which is supported by the present DNA comet data (Fig. 1). The group supplemented with tea extract shown a limited but considerable protection, while the arsenic group's cytoplasm displayed vacuolar degeneration, karyolysis, and karyorrhexis.[13] Ghost cells in the arsenic-treated group were significant (39%) and recovered to 12% in the tea-supplemented group. This corresponds to the comet's head and tail measurements (Fig. 1). Our rat experiment further suggests that tea can restore AChE activity and postural imbalance in rats.

In summary the brief mechanistic steps may be written as such: a) AChE ↑ → Ghost Cells ↑ (positive correlation), b) AChE ↑ → Recovery Score ↓ (negative correlation) c) Ghost Cells ↑ → Recovery Score ↓ (negative correlation).

In critical analysis the theaflavin inhibition of AChE may represented by the dose-response curve: % AChE inhibition *vs* log concentration which is included in (Fig. 1) as $R^2 = 0.991$ annotations. Mechanistic inset of enzymatic inhibition shows mixed-type inhibition: E + S ↔ ES → E + P, E + I ↔ EI and ESI.

Acetylcholinesterase inhibition study with a purified enzyme

AChE was dose-dependently suppressed by every investigated drug (Suppl. Fig. S1). Pure AChE was more significantly inhibited by theaflavin compounds than by any other catechin (Table 1). Black tea extracts had a lower IC_{50} value than green tea (Suppl. Fig. S2). The molecular docking pictures are shown in (Suppl. Fig. S2). All galloylated catechins showed more inhibitory action than non-galloylated catechins.

The ECG showed the most inhibition activity among the catechins (IC_{50}= 17.91±0.8 µg/mL (41 µM) (Table 1). However, Theaflavin digallate (TFDG) and Theaflavin monogallate (TFMG) showed highly promising inhibitory effects with IC_{50} of 1.45 ± 0.06 µg/mL (1.6 µM) and 2.38 ± 0.08 µg/mL (3.3 µM), respectively. Gallic acid was thought to play a major role in AChE enzyme inhibitory action because all galloylated phytochemical compounds showed promising inhibition which is supported by Okello *et al*. 2012[23].

Acetylcholinesterase inhibition kinetics

Because of their efficacy, TFs and its derivatives (TFMG and TFDG) were used in the AChE inhibition kinetic study (Table 1). The lower atomic contact energy values (ACE, -369 to -287 kcal/mol) of the molecular docking experiments (Table 1) confirm the lower IC50 values of TFMG and TFDG (Fig. 1), which indicate their high interactability with the enzyme. In the presence of the inhibitors TFDG, TFMG, and TF, it was found that the Km,app and Vmax,app values of AChE reduced; these values further fell as the inhibitor concentration increased (Fig. 1 & Table 2). The unusual mixed-type and noncompetitive-uncompetitive inhibition of the AChE enzyme was caused by TFDG, TFMG, and TF. As the inhibitor concentration rose, as was previously seen, the Km, app, and Vmax, app values fell in this case[24]. The kinetics parameters suggest that all theaflavins might bind other than substrate-binding site of AChE and inhibit product-release. This inhibition-kinetics is supported by our molecular-docking study (Table 1), where TFDG and TFMG prefer to bind docking site S_2 rather than site S_1.

Table 1 — Acetylcholinesterase inhibitory activities (IC_{50}) and bioinformatic result atomic contact energy values (ACE of 2 docking sites) of selected tea phytochemicals

Compound Name	IC_{50} (µg/ml)[a]	Docking Site 1	Docking Site 2
		ACE Value (No. of docking sites 20)(kcal/mol)	
EGCG	30.99 ± 1.5 (67 µM)	-140.72 (2)	-298.08 (7)
GCG	25.83 ± 1.1 (54 µM)	-152.56 (1)	-280.61 (8)
ECG	17.91 ± 0.8 (41 µM)	-170.27 (3)	-314.07 (7)
CG	21.31 ± 0.7 (49 µM)	-160.44 (2)	-287.69 (6)
EC	81.97 ± 2.5 (282 µM)	-	-240.29 (10)
EGC	76.68 ± 1.6 (250 µM)	-	-212.74 (9)
Gallic acid	483.36 ± 15.3 (2.84 mM)	-	-
TF	16.64 ± 0.4 (29 µM)	-284.66 (2)	-300.44 (4)
TFMG	2.38 ± 0.08 (3.3 µM)	-287.03 (5)	-347.06 (3)
TFDG	1.45 ± 0.06 (1.6 µM)	-344.71 (5)	-369.87 (5)
Eserine salicylate[b]	1.30 ± 0.06 (3.1 µM)	-	-

Table 2 — Kinetic parameters of AChE in presence and absence of inhibitors. [I] (inhibitor concentration) is expressed in μM, V_{max} (and or $V_{max,app}$in presence of inhibitor)in μM /min, K_m (and or $K_{m,app}$in presence of inhibitor) in μM, K_{cat} in s^{-1}, K_{cat}/K_m in s^{-1} μM^{-1}, K_i in μM, K_{ia} represents the dissociation constant for Enzyme -Inhibitor complex (EI), K_{ib} represents the dissociation constant for Enzyme-Substrate-Inhibitor complex (ESI)

Inhibitor	[I]	V_{max} or $V_{max, app}$	K_m or $K_{m, app}$	K_{cat}	K_{cat}/K_m	K_i	Inhibition type
No inhibitor	0	8.06	65.86	1.34×10^4	204.06	-	-
TFDG	2.5	3.62	41.45	0.60×10^4	145.55	K_{ia}, 2.03 K_{ib} 6.22	Mixed type
	5.0	2.97	36.43	0.49×10^4	135.88	K_{ia}, 2.91 K_{ib} 9.96	
TFMG	2.5	4.48	45.47	0.75×10^4	164.21	K_{ia}, 3.12 K_{ib} 10.30	Mixed type
	5.0	3.70	41.59	0.62×10^4	148.27	K_{ia}, 4.23 K_{ib} 13.29	
TF	2.5	6.53	61.94	1.09×10^4	175.71	K_{ia}, 10.64 K_{ib} 15.49	Mixed type
	5.0	5.84	57.66	0.97×10^4	168.81	K_{ia}, 13.12 K_{ib} 23.94	

***Molecular docking* study**

The binding site of AChE consists of multiple pockets and those are involved in catalytic mechanism, product formation/release. These pockets include the acyl pocket, oxyanion hole, catalytic (CAT), anionic site, and peripheral anionic site (PAS). These locations display distinct representations of amino acids and serve three different purposes. Of them, the 20 Å long internal grove's most external location is the Peripheral Anionic Site (PAS) (designated as Site 2 in the current study)[25]. The substrate's acyl group is bound by the Acyl pocket, also known as the Acyl-subsite (AS), which is denoted by PHE297, PHE295 and PHE338. The substrate is then oriented toward the catalytic triad (HIS447, GLU334 and SER203) behind the AS. Both subsites are commonly called catalytic anionic subsite. According to one report GLY122 of oxyanion hole maintains the function of acyl pocket (AS) neutralizing steric hindrance[26].

According to the present study on molecular docking between acetylcholine and acetylcholinesterase (PDB ID: 4M0E)[27] two consecutive sites were found which demonstrated the entry of acetylcholine within 20 Å long internal grove and movement towards the catalytic site respectively (Fig. 2a & b). Two consequent binding sites 1 and 2 were determined by Sussman *et al*., 1991 in AChE from the electric organ of *Torpedo californica* by x-ray analysis to 2.8 angstrom resolution[28]. Acetylcholine establishes a hydrogen bond with the enzyme's surface amino acid, HIS 405: HD1 (H bond length: 1.861Å, binding energy: 3.39kCal/mol), at docking site 1 (Fig. 2a). From there, it travels to the docking subsite at the inner location of the enzyme. At that location, a hydrogen bond between acetylcholine and SER203 was seen (H bond length: 2.05Å, binding energy: -3.99 kCal/mol) (Fig. 2b). Radic *et al*. (1993) showed during the butyrylcholinesterase inhibition investigation a unique pocket of binding with three distinct domains[29]. This report demonstrates that all of the three domains are composed of a cluster of aromatic amino acid residues[29].

According to earlier research, acetylcholinesterase's substrate is dihydrotanshinone[30]. As seen in Figure 2c, dihydrotanshinone interacted with the often reported amino acids at the PAS, ES, and AS sites in the X-ray diffraction structure of 4M0E. Blind docking is required to determine the inhibitor's affinity for a predefined active site. The non-specified, overall docking or blind molecular docking with dihydrotanshinone also showed the common interaction pattern with TRP286, TYR124, PHE297, PHE295, TYR337 and TYR341 with a lowest binding and final internal energy value of -8.84 kcal/mol (Fig. 2d). In contrast, eserine had the lowest binding energy value of -7.85 kCal/mol and the final internal energy value of -8.45 kcal/mol when it interacted with the same amino acids, namely TRP286, PHE297, and TYR341 (Fig. 2e). Their greatest affinity was also demonstrated by blind docking with TFMG and TFDG to site 2, which includes PAS, ES, AS, and the catalytic triad site (Suppl. Fig. S3).

Among them TFMG showed the highest affinity with acetylcholinesterase (Binding energy: -9.84kCal/mol, final intermolecular energy: -11.41 kcal/mol) (Suppl. Fig. S3).

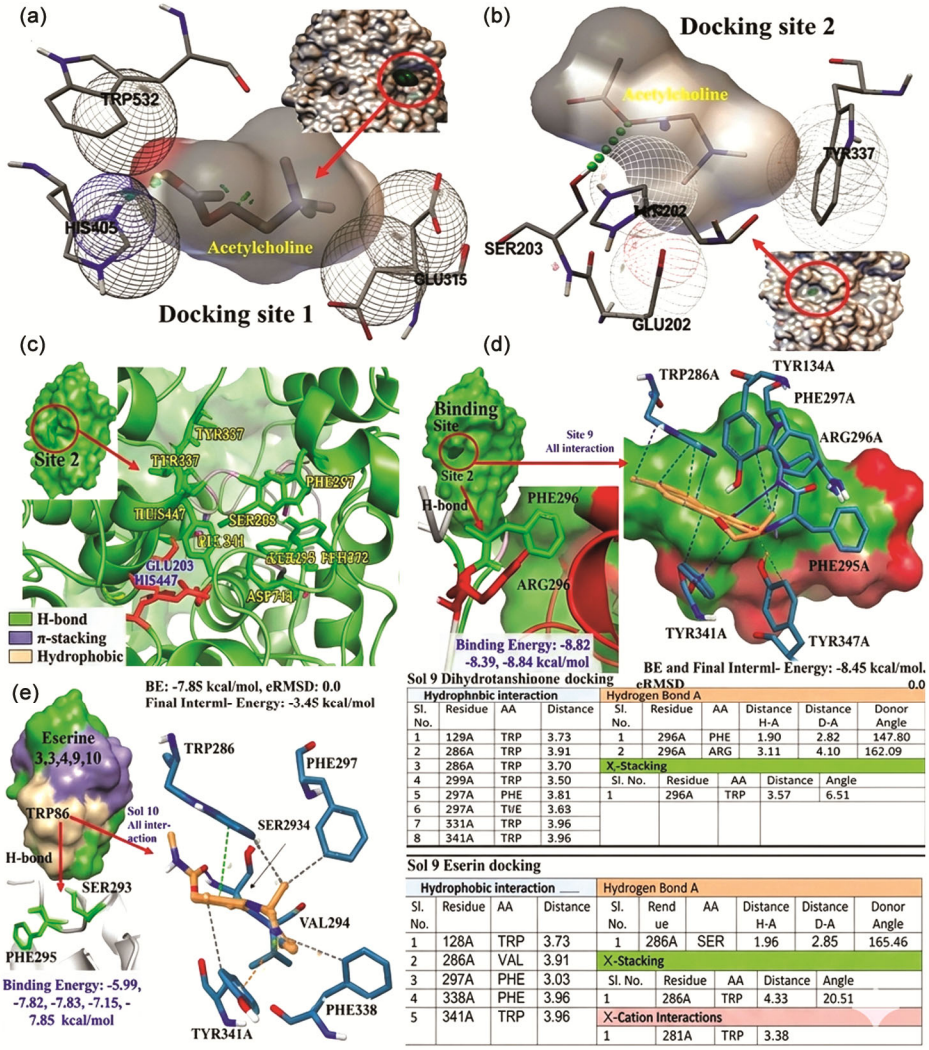

Sol 9 Dihydrotanshinone docking eRMSD 0.0

Hydrophnbic interaction				Hydrogen Bond A					
Sl. No.	Residue	AA	Distance	Sl. No.	Residue	AA	Distance H-A	Distance D-A	Donor Angle
1	129A	TRP	3.73	1	296A	PHE	1.90	2.82	147.80
2	286A	TRP	3.91	2	296A	ARG	3.11	4.10	162.09
3	286A	TRP	3.70	X-Stacking					
4	299A	TRP	3.50	Sl. No.	Residue	AA	Distance	Angle	
5	297A	PHE	3.81	1	296A	TRP	3.57	6.51	
6	297A	TYR	3.63						
7	331A	TRP	3.96						
8	341A	TRP	3.96						

Sol 9 Eserin docking

Hydrophobic interaction				Hydrogen Bond A					
Sl. No.	Residue	AA	Distance	Sl. No.	Rend ue	AA	Distance H-A	Distance D-A	Donor Angle
1	128A	TRP	3.73	1	286A	SER	1.96	2.85	165.46
2	286A	VAL	3.91	X-Stacking					
3	297A	PHE	3.03	Sl. No.	Residue	AA	Distance	Angle	
4	338A	PHE	3.96	1	286A	TRP	4.33	20.51	
5	341A	TRP	3.96	X-Cation Interactions					
				1	281A	TRP	3.38		

Fig. 2 — (a) Hydrogen bonding between acetylcholine and HIS405 at Site1; (b) hydrogen bonding between acetylcholine and SER203 at Site2. (c) The green marked amino acids were the active molecules of PAS and ES and red amino acids were associated with catalytic site. (d) Molecular docking with dihydrotanshinone showed interactions with the lowest binding energy value of -8.84 kCal/mol. (e) The positive control inhibitor Eserine showed interaction with the same active site with the lowest binding energy value of -7.85 kCal/mol

Molecular dynamic simulation study

Lower RMSD values indicated heightened stability, signifying minimal divergence from the initial configuration. Conversely, RMSF values provided essential insights into the fluctuations exhibited by individual atoms within the systems. Higher structural rigidity was indicated by lower atomic fluctuations, which were shown by reduced RMSF values. We determined that the best fit was the acetylcholinesterase with theaflavin monogallate and digallate complex system (Fig. 3). This system in particular had the lowest RMSD and RMSF values, indicating the least amount of atomic fluctuations and minimum departure from its starting state.

Energy analysis

Docked complex of acetylcholinesterase (PDB ID: 4M0E) and Theaflavin monogallate resulted Δ*G -9.1* (Fig. 4). The docking complex resulted total 19 amino acids interacted with ligand molecule. Docked complex of acetylcholinesterase (PDB ID: 4M0E) and Theaflavin digallate resulted Δ*G -9.3* (Fig. 4). The docking complex resulted total 23 amino acids interacted with ligand molecule. TFDG was also found to interact with the common amino acids *i.e.* TRP286, PHE295 and TYR341 (Fig. 3). Moreover, The 20 Å long internal grove of the active site is also linked to the SER293, THR75, and TYR72, with which it bound (Suppl. Fig. S3 & Fig. 3) and (Suppl. Table S1-S5). In addition to being larger than

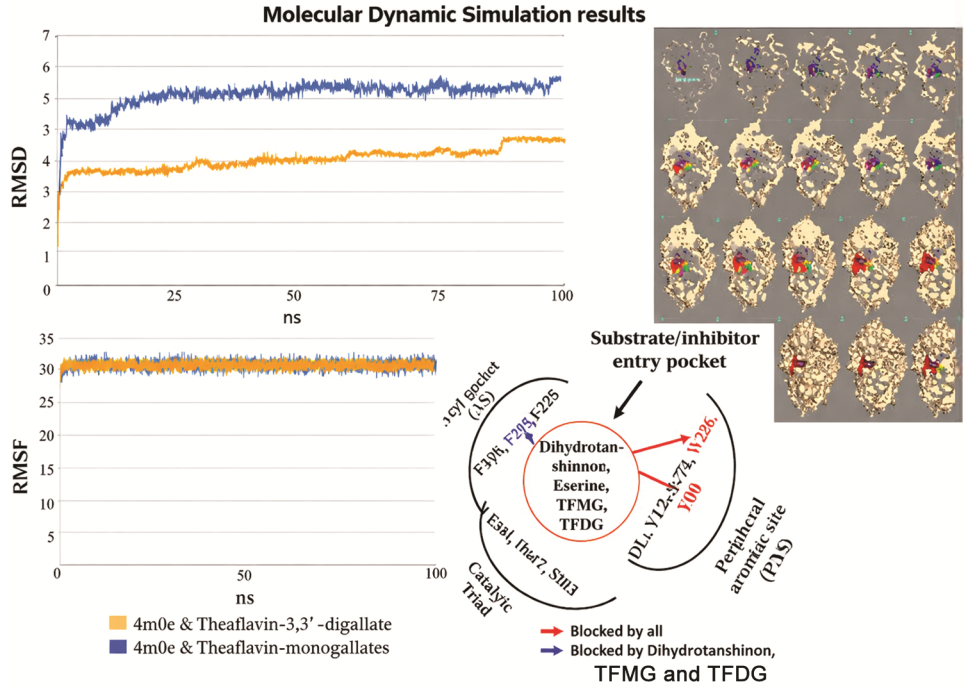

Fig. 3 — Molecular Dynamic simulation analysis evaluated the root mean square deviation (RMSD) and root mean square fluctuation (RMSF) of the docked complexes of AChE and TFMG and AChE and TFDG. Summarization picture represents gradual occupancy of theaflavin gallate to the target site of AChE. The common pockets *i.e.* entry pocket, acyl pocket where the catalytic triad is formed in the Site 2 are shown. TFMG, TFDG and serine salicylate and dihydrotanshinone differentially interacts with preferred amino acids. Amino acids W286 and Y341 were blocked by all but F295 was blocked by substrate dihydrotanshinone and inhibitors TFMG and TFDG

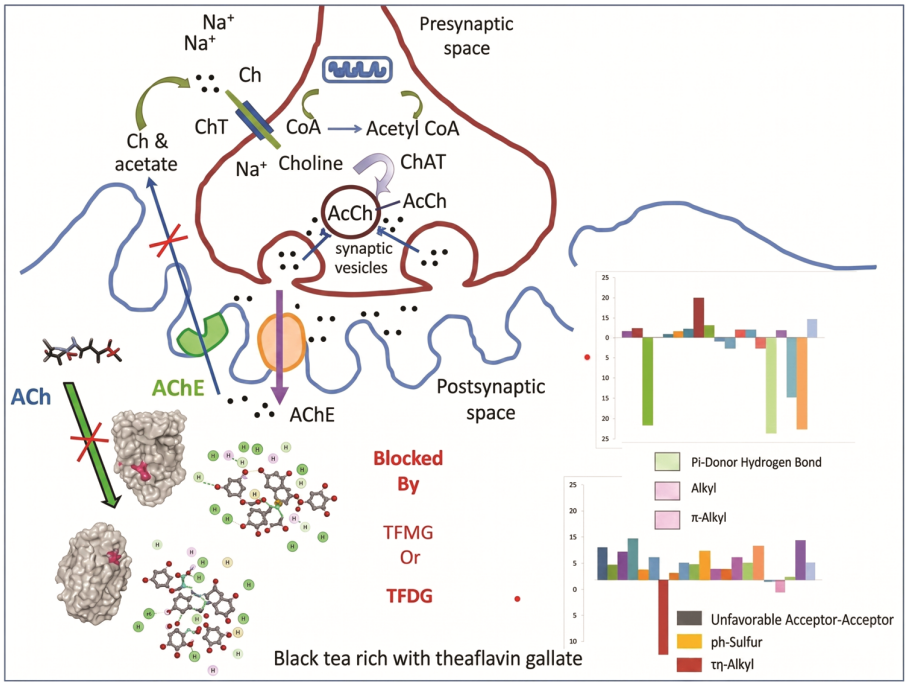

Fig 4 — demonstrates the blocking effects of theaflavin gallates on AChE in the post synaptic space in the neuromuscular junction. Theaflavin gallates inhibits the AChE by restricting the entry of its substrate, ACh to the binding-catalytic site of the enzyme. Interatomic profile and energy distribution of acetylcholinesterase with Theaflavin mono-gallate or di-gallate docked complexes are shown in the bottom panel. Bar graphs demonstrate the energy distribution of amino acids interacted with ligand molecules

dihydrotanshinone (bottom panel tabulation of Fig. 2 and Suppl. Fig. S3), TFMG has the highest inhibitory efficiency from an interaction perspective (61.15 nM). It also totally blocks the hallmark amino acids at the catalytic site (Fig. 3). Our current result is supporting to the outcome of ACE data that basically reflect the findings of the *in vivo* study.

With the lowest RMSD and RMSF values of any system, the acetylcholinesterase with theaflavin digallate and theaflavin monogallate complex demonstrated exceptional stability and low atomic fluctuations. This explains why theaflavin gallate interacts with AChE more effectively by creating hydrogen and hydrophobic interactions[31]. Thus, bioavailability of these compounds might be raised in lipid-rich brain tissues and during bi-layer membrane transport. Positive ΔH and ΔS values show that van der Waals and hydrophobic forces promote the spontaneous binding of flavones to proteins. Potentially for the optimal binding adjustment, TFMG lowered the α-helix and increased the β-sheet in the secondary structure of proteins[32]. Because of their accessibility to ligands and solvents, the pockets of the AChE protein interact more than the cavities. In general, pocket sharing is important from a pharmacological perspective. From a stereochemical standpoint, theaflavin-gallate is more favorable than other gallates and catechins since it contains five rotatable bonds and occupies four different plains[33].

AChE activity is compromised in neuro-muscular degeneration, poisoning consequences, and chronic arsenic exposure. Numerous data indicate that neuronal and neuromuscular breakdown occurs when cholinergic processes are impaired. Inflammation, oxidative stress, and other factors encourage this. Higher AChE activity frequently leads to decreased cholinergic stimulation and related problems. So, we can summarize the arsenic toxicity steps and neuromuscular protection by theaflavin as follows: a) Arsenic Toxicity Pathway: Arsenic Exposure → ↑ AChE Activity → Neuronal Damage. b) AChE Inhibition → ↓ Neuronal Damage → Restoration of Normal Morphology.

Conclusion

In the current *in vitro*, *in vivo* and MD simulation studies, we demonstrated that TF, TFMG and TFDG inhibit the AChE activity and this inhibition occurs in dose-dependent noncompetitive-uncompetitive and with mixed-type manner. Out of the studied compounds, TFMG and TFDG showed promising inhibition of AChE activity. Further studies are necessary in this regard.

Acknowledgement

The authors are thankful to Bijoy Chandra Ghosh, former professor of Agricultural and Food Engineering Department, Indian Institute of Technology Kharagpur, for providing the tea samples.

Conflicts of interest

All authors declare no conflicts of interest.

References

1 Soreq H & Seidman S, Acetylcholinesterase — new roles for an old actor. *Nat Rev Neurosci,* 2 (2001) 294.

2 Francis PT, Palmer AM, Snape M & Wilcock GK, The cholinergic hypothesis of Alzheimer's disease: a review of progress. *J Neurol Neurosurg Psychiatry,* 66 (1999) 137–147.

3 Kar S, Slowikowski SP, Westaway D & Mount HT, Interactions between β-amyloid and central cholinergic neurons: implications for Alzheimer's disease. *J Psychiatry Neurosci,* 29 (2004) 427.

4 Trang A & Khandhar PB, Physiology, Acetylcholinesterase. In: *StatPearls [Internet]*. Treasure Island (FL): StatPearls Publishing; 2025 Jan.

5 Walczak-Nowicka ŁJ & Herbet M, Acetylcholinesterase inhibitors in the treatment of neurodegenerative diseases and the role of acetylcholinesterase in their pathogenesis. *Int J Mol Sci,* 22 (2021) 9290.

6 McHardy SF, Wang HL, McCowen SV & Valdez MC, Recent advances in acetylcholinesterase inhibitors and reactivators: an update on the patent literature (2012–2015). *Expert Opin Ther Pat,* 27 (2017) 455.

7 Jackisch R, Förster S, Kammerer M, Rothmaier AK, Ehret A, Zentner J & Feuerstein TJ, Inhibitory potency of choline esterase inhibitors on acetylcholine release and choline esterase activity in fresh specimens of human and rat neocortex. *J Alzheimers Dis,* 16 (2009) 635.

8 Muramatsu I, Uwada J, Yoshiki H, Sada K, Lee KS, Yazawa T, Taniguchi T, Nishio M, Ishibashi T & Masuoka T, Novel regulatory systems for acetylcholine release in rat striatum and anti-Alzheimer's disease drugs. *J Neurochem,* 149 (2019) 605.

9 Colović MB, Krstić DZ, Lazarević-Pašti TD, Bondžić AM & Vasić VM, Acetylcholinesterase inhibitors: pharmacology and toxicology. *Curr Neuropharmacol,* 11 (2013) 315.

10 Perry NS, Bollen C, Perry EK & Ballard C, Salvia for dementia therapy: review of pharmacological activity and pilot tolerability clinical trial. *Pharmacol Biochem Behav,* 75 (2003) 651.

11 Medda N, Patra R, Ghosh TK & Maiti S, Neurotoxic mechanism of arsenic: synergistic effect of mitochondrial instability, oxidative stress, and hormonal-neurotransmitter impairment. *Biol Trace Elem Res,* 198 (2020) 8.

12 Mochizuki H, Phyu KP, Aung MN, Zin PW, Yano Y, Myint MZ, Thit WM, Yamamoto Y, Hishikawa Y, Thant KZ, Maruyama M & Kuroda Y, Peripheral neuropathy induced by drinking water contaminated with low-dose arsenic in Myanmar. *Environ Health Prev Med,* 24 (2019) 23.
13 Maiti S, Acharyya N, Ghosh TK, Ali SS, Manna E, Nazmeen A & Sinha NK, Green tea (*Camellia sinensis*) protects against arsenic neurotoxicity via antioxidative mechanism and activation of superoxide dismutase activity. *Cent Nerv Syst Agents Med Chem,* 17 (2017) 187.
14 Roy S, Chattoraj A & Bhattacharya S, Arsenic-induced changes in optic tectal histoarchitecture and acetylcholinesterase–acetylcholine profile in *Channa punctatus*: amelioration by selenium. *Comp Biochem Physiol C Toxicol Pharmacol,* 144 (2006) 16.
15 Sharma VK, Bhattacharya A, Kumar A & Sharma HK, Health benefits of tea consumption. *Trop J Pharm Res,* 6 (2007) 785.
16 Graham HN, Green tea composition, consumption and polyphenol chemistry. *Prev Med,* 21 (1992) 334.
17 Acharyya N, Chattopadhyay S & Maiti S, Chemoprevention against arsenic-induced mutagenic DNA breakage and apoptotic liver damage in rat via antioxidant and SOD1 upregulation by green tea (*Camellia sinensis*). *J Environ Sci Health C Environ Carcinog Ecotoxicol Rev,* 32 (2014) 338.
18 Tarhoni MH, Vigneswara V, Smith M, Anderson S, Wigmore P, Lees J, Ray DE & Carter WG, Detection, quantification and microlocalisation of targets of pesticides using microchannel plate autoradiographic imagers. *Molecules,* 16 (2011) 8535.
19 Moon UR, Sen SK & Mitra A, Antioxidant capacities and acetylcholinesterase-inhibitory activity of *Hoppea fastigiata*. *J Herbs Spic Med Plants,* 20 (2014) 115.
20 Bjelkmar P, Larsson P, Cuendet MA, Hess B & Lindahl E, Implementation of the CHARMM force field in GROMACS: analysis of protein stability effects from correction maps, virtual interaction sites, and water models. *J Chem Theory Comput,* 6 (2010) 459.
21 GROMACS Development Team, *GROMACS Documentation Release 2021.2.*
22 Guex N & Peitsch MC, SWISS-MODEL and the Swiss-Pdb Viewer: an environment for comparative protein modeling. *Electrophoresis,* 18 (1997) 2714.
23 Okello EJ, Leylabib R & McDougall GJ, Inhibition of acetylcholinesterase by green and white tea and their simulated intestinal metabolites. *Food Funct,* 3 (2012) 651.
24 Moon UR, Sircar D, Barthwal R, Sen SK, Beuerle T, Beerhues L & Mitra A, Shoot cultures of *Hoppea fastigiata* (Griseb.) C.B. Clarke as potential source of neuroprotective xanthones. *J Nat Med,* 69 (2015) 375.
25 Ordentlich A, Barak D, Kronman C, Flashner Y, Leitner M, Segall Y, Ariel N, Cohen S, Velan B & Shafferman A, Dissection of the human acetylcholinesterase active center determinants of substrate specificity. *J Biol Chem,* 268 (1993) 17083.
26 Ordentlich A, Barak D, Kronman C, Ariel N, Segall Y, Velan B & Shafferman A, Functional characteristics of the oxyanion hole in human acetylcholinesterase. *J Biol Chem,* 273 (1998) 19509.
27 Cheung J, Gary EN, Shiomi K & Rosenberry TL, Structures of human acetylcholinesterase bound to dihydrotanshinone I and territrem B show peripheral site flexibility. *ACS Med Chem Lett*, 4 (2013) 1091.
28 Sussman JL, Harel M, Frolow F, Oefner C, Goldman A, Toker L & Silman I, Atomic structure of acetylcholinesterase from *Torpedo californica*: a prototypic acetylcholine-binding protein. *Science,* 253 (1991) 872.
29 Radić Z, Pickering NA, Vellom DC, Camp S & Taylor P, Three distinct domains in the cholinesterase molecule confer selectivity for acetyl- and butyrylcholinesterase inhibitors. *Biochemistry,* 32 (1993) 12074.
30 Cheung J, Rudolph MJ, Burshteyn F, Cassidy MS, Gary EN, Love J, Franklin MC & Height JJ, Structures of human acetylcholinesterase in complex with pharmacologically important ligands. *J Med Chem,* 55 (2012) 10282.
31 Lei S, Xu D, Saeeduddin M & Riaz A, Characterization of molecular structures of theaflavins and interactions with bovine serum albumin. *J Food Sci Technol,* 54 (2017) 3421.
32 Xu D, Wang Q, Zhang W, Bing H, Li Z, Zeng XX & Sun Y, Inhibitory activities of caffeoylquinic acid derivatives from *Ilex kudingcha* C.J. Tseng on α-glucosidase from *Saccharomyces cerevisiae*. *J Agric Food Chem,* 63 (2015) 3694.
33 Maiti S, Banerjee A & Kanwar M, Effects of theaflavin-gallate *in silico* binding with different proteins of SARS-CoV-2 and host inflammation and vasoregulations referring an experimental rat-lung injury. *Phytomed Plus,* 2 (2022) 100237.